IEEE Access
Multidisciplinary | Rapid Review | Open Access Journal

Received October 4, 2017, accepted October 31, 2017, date of publication November 8, 2017, date of current version December 5, 2017.

Digital Object Identifier 10.1109/ACCESS.2017.2771494

Early-Warning System With Quasi-Distributed Fiber Optic Sensor Networks and Cloud Computing for Soil Slopes

DONG-SHENG XU[1], LONG-JUN DONG[2], (Member, IEEE), LALIT BORANA[3], AND HUA-BEI LIU[1]

[1]School of Civil Engineering and Mechanics, Huazhong University of Science and Technology, Wuhan 430074, China
[2]School of Resources and Safety Engineering, Central South University, Changsha 410083, China
[3]Department of Civil Engineering, IIT Indore, Indore 453552, India

Corresponding author: Long-Jun Dong (lj.dong@csu.edu.cn)

This work was supported in part by the National Natural Science Foundation of China under Grant 51508215 and Grant 41672277, in part by the Fundamental Research Funds for Central Universities of China under Grant 2017KFYXJJ138, in part by the Young Elite Scientists Sponsorship Program by CAST under Grant 2016QNRC001, and in part by the Innovation-Driven Project of Central South University under Grant 2016CXS001.

ABSTRACT Slope failure and debris flow cause lots of casualties and property loss. An early-warning system for slope collapse and debris flow is essential to ensure safety of human beings and assets. Based on fiber optic sensing technology and Internet of Things, a new sensing transducer for internal earth pressure measurement in a soil slope is proposed, fabricated, and tested in this paper. The working principles, theoretical analysis, laboratory calibrations, and discussions of the proposed pressure transducers are elaborated. Extensive evaluations of the resolutions, physical properties, and response to the applied pressures have been performed through modeling and experimentations. The results show that the sensitivity of the designed pressure sensor is 0.1287 kPa/$\mu\varepsilon$ across a pressure range of 140 kPa. Finally, a field soil slope was instrumented with the developed fiber optic sensors and other sensors. Through internet and cloud computing platform, the stability of the soil slope was analyzed. In the cloud computing platform, the numerical simulation is carried out by considering the slope internal deformations, rainfall infiltration, and limit force equilibrium. The factor of safety of the soil slope was calculated, which could be used to determine health condition of the instrumented slope. The performance was evaluated and classified into three categories. It proves that the proposed early-warning system has potential to monitor the health condition of the soil slopes.

INDEX TERMS Fiber optic sensor, Internet of Thing, cloud computing, early-warning system, slope.

I. INTRODUCTION

In recent decades, there has been rapid modernization, industrialization and infrastructural development across the world. The stability of soil slopes is a big concern in crowded city for civil engineers. Slope collapse and rainfall infiltration will result in debris flow which will cause large casualties and property losses. Thus, there is a desire need of early-warning systems for large-scale soil slopes in crowded cities.

Many early warning systems have been developed in the literature, such as Zan *et al.* [1] presented an early warning system with laser displacement. Dong *et al.* [2] reported a pre-alarm system with coupled model of Gray and Generalized Regression Neural Network for a tailings dam in mines. In the early-warning system, the sensing transducer is the most important part, as it will obtain raw data in the instrumented object. For a soil slope, the material different from waters or liquid, concrete, and steel materials, it contents various gravel particles with various dimensions and shapes. Thus, the measurement of earth pressure in gravel material is difficult than that in the water. Normally, the earth pressure induced by the gravel particles can be divided into two parts: normal pressure and shear pressure. The shear pressure can be calculated though poison's ratio, thus the normal pressure is a concern for civil engineers. In the paper, the term of earth pressure means the average normal pressure over a range of gravel particles.

Conventional pressure sensors, such as radar beam, magnetic floating, air purging type sensors and system based on strain gauges, vibration wires and other electric signals have been widely utilized to measure the earth pressures or water pressures [3], [4]. However, the pressure sensors based on electric signals have limitations of corrosion and electromagnetic interference problems. In recent years, the development of micro-electro-mechanical systems (MEMS) has gained extensive attentions. Many pressure sensors based on MEMS have been developed, such as a rigid-electrode with deformable membrane [5] and a mechanical force displacement transduction structure of MEMS pressure sensors were developed [6]. Shahiri-Tabarestani *et al* [7]. proposed a slotted diaphragm for a capacitive pressure sensor. A double deformable diaphragm was also used for the MEMS pressure sensors [8]. Even though the MEMS pressure sensor has tiny size and good accuracy, it has difficult to be applied for earth pressure measurement due to the earth material contents of many gravel particles. The pressure sensor should have the capacity of measuring a wide range of gravel particles.

With the development of fiber optic sensing (FOS) technology, many researches have been conducted to demonstrate the application of FOS in pressure measurement. As compared with the conventional electrical sensing technology, the fiber optic sensing technology has many intrinsic advantages, such as corrosion resistance, resistance to electromagnetic interference (EMI), high resolution and precision, small size, large bandwidth and multiplexing ability [9]–[11]. Some researchers have proposed Fiber Bragg Grating (FBG) based pressure sensors for monitoring liquid level [12]–[14]. Yang *et al.* [15] demonstrated the successful application of a multiplexed array of fiber optic liquid-level point sensors in a cryogenic environment. Researches have demonstrated the simultaneous measurement of pressure (up to 30 MPa) and temperature (up to 430 °C) by fiber optic Extrinsic Fabry-Perot interferometer (FP) sensor [16], [17]. It is also noted that the fiber sensors can be used to monitor the pressure up to 70 MPa under isothermal conditions [18].

In this study, an early warning system can be established for a soil slope with fiber optic sensing technologies, the sensor data interpretation [19]–[21], the internet of things (IoT) [22], cloud computing [23] and wireless sensor networks [24]–[26]. Firstly, an early-alarm system for real-time motoring of soil slopes is presented with four layers, such as a sensing layer, an IoT layer, a cloud computing layer and an application layer. In the sensing layer, a new type of fiber-optic based pressure sensor (FPS) for pressure measurement of earth materials is proposed, fabricated and analyzed. The working principles, fabricated details and calibration tests are elaborated. A series of experimental tests have been performed to examine the relationship between applied pressures and strains induced in FBG sensors. Finally, the early-warning system was applied in a field soil slope. With the numerical simulation and slope stability analysis, the health condition of the instrumented slope was evaluated. The health condition was classified into three categories and used for the application layer.

II. THE HIERARCHICAL STRUCTURE OF EARLY-ALARM SYSTEM

An early-alarm system for real-time monitoring of soil stability is essential to reduce or avoid casualties and property losses for debris flow. The alarm system based on real-time monitoring data from fiber-optic sensors and numerical analysis using cloud computing for soil slopes. The hierarchical structure of the early-alarm system is shown in Fig. 1. As indicated in the figure, the system consists of four layers, which are a sensing layer, an IOT layer, the cloud computing layer and the application layer.

A. THE SENSING LAYER OF INSTRUMENTATIONS

The sensing layer is a most fundament layer in the whole early-warm system, as the further analysis and numerical simulation are based on the measured data. The sensing layer consists of various fiber optic sensors which can be connected in series with a single fiber. Fig. 2 shows the working principle of the single-mode FBG sensors, in which a broadband light source transmitted through the FBG sensor, and a narrow band of light is reflected. The reflected wavelength λ_B has a relation to the core index of refraction and the grating period of the index modulation, which is expressed as follows:

$$\lambda_B = 2n_{eff}\Lambda \tag{1}$$

where n_{eff} is the core index of refraction and Λ is the grating period of index modulation. The reflected wavelength λ_B varied with the local strains and temperatures. The changed wavelength $\Delta\lambda_B$ induced by strain and temperature is given by [10]:

$$\frac{\Delta\lambda_B}{\lambda_B} = (1 - p_e)\,\varepsilon + (\alpha_e + \xi_e) = c_1\varepsilon + c_2\Delta T \tag{2}$$

where λ_B is the initial Bragg's wavelength; $\Delta\lambda_B$ is a shift in the Bragg's wavelength; p_e is the photo elastic coefficient; α_e and ξ_e are the coefficients of temperature effect; ΔT is the change of temperature; c_1 and c_2 are the coefficients related to strain and temperature variations, respectively; $c_1 = 0.78 \times 10^{-6}/\mu\varepsilon$ and $c_2 = 6.67 \times 10^{-6}/°\text{C}$. In this study, the FBG sensor has wavelength ranges from 1510 nm to 1590 nm. The Bragg length of each FBG sensor is 6 mm. The FBG sensor was fabricated by adopting the phase mask method based on a single mode optical fiber and following the guidelines as articulated by Xu [27]. Briefly, the whole fabrication procedures for the FBG sensor can be divided into three stages: (a) preparation of the photosensitive optical fiber, (b) creating a Bragg grating using the phase mask method, and (c) thermal annealing [27]. The FBG sensing interrogator is SM125 from Micron Optics which has a wavelength resolution of 1 pm. By substituting to the Eq. 2, the strain measurement resolution of the FBG sensor is around $1\mu\varepsilon$.

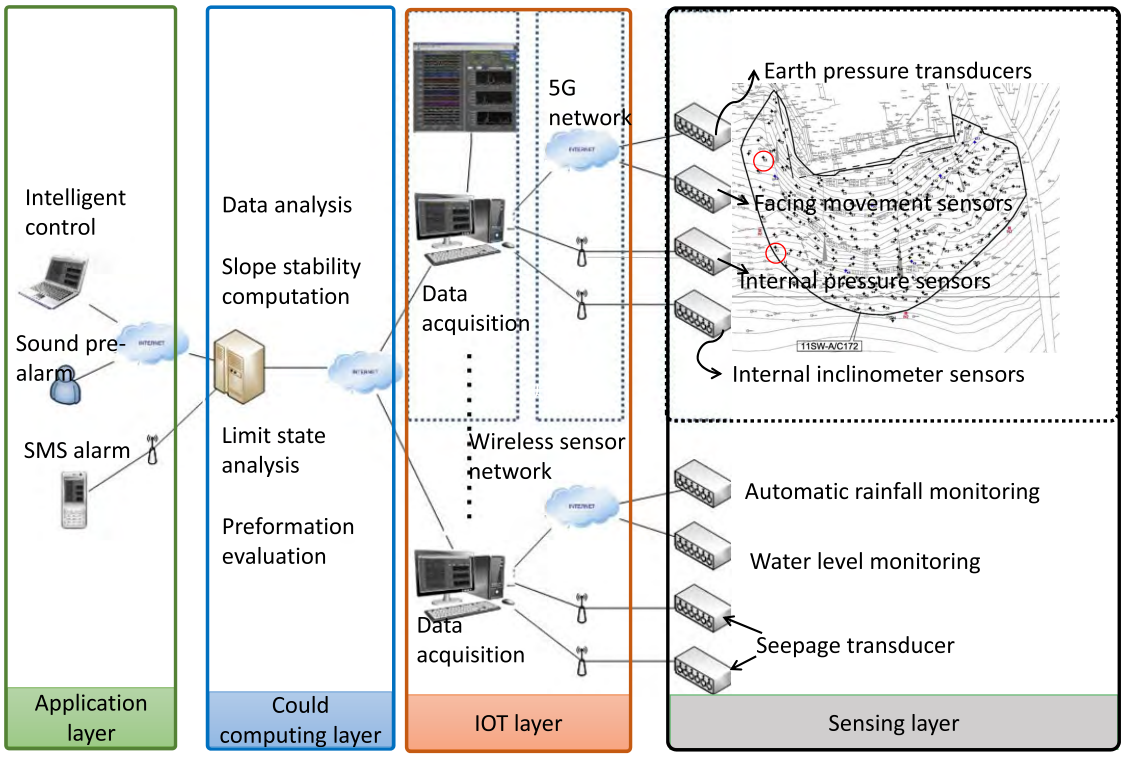

FIGURE 1. The hierarchical structure of early-alarm system for soil slope.

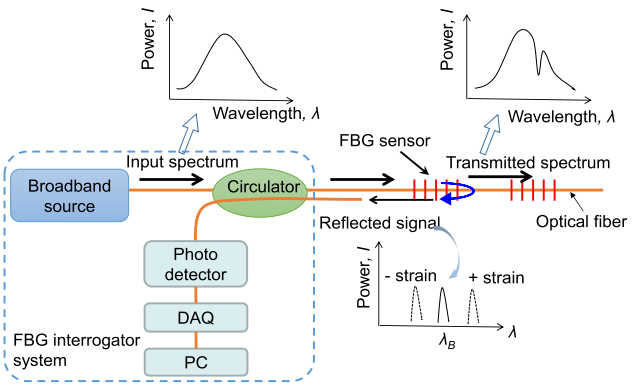

FIGURE 2. Working principle of the fiber-optic Bragg sensors.

B. THE IoT LAYER

The IoT layer includes data acquisition system, fiber optic sensing interrogator, distributed sensors, wireless network, and remote control. All fiber optic transducers will be connected with the fiber optic sensing interrogator through an armed optical fiber. The wavelength information will be obtained in real-time to monitor the surrounding deformations, internal soil stresses, temperatures and rainfall data. These data will be recorded by the data acquisition system. All the data will be uploaded to the cloud computing platform through wireless network or wireless network. The instructions for sensing layer can be also downed from the cloud computing platform. The wireless network and wireless network can improve the data transmission through sensing layer and cloud computing layer, which is essential for the real-time monitoring and early-warm of debris flows.

C. THE CLOUD COMPUTING LAYER

The cloud computing layer includes data classifications, sensor data evaluation, numerical modeling, slope stability analysis, and risk evaluations. First of all, the data transmitted from the IoT layer will be classified and examined. The error data will be determined and excluded. Secondly, the transducer data will be classified in different categories, such as deformation, stress, temperature, seepage and factor of safety (FOS). Finally, the data will be combined in a numerical model to analyze the safety levels. A safety indicator will be yield from the cloud computing layer.

D. THE APPLICATION LAYER

Fig. 3 shows the real-time early-alarm system for debris flow. The application layer is the top layer of the whole early-warning system. The application layer is direct to the ender users and based on the IoT, cloud computing and numerical analysis. The application layer aims to send the stability information of slopes to ender users through various methods, such as sound-light alarm system, SMS, emails, and emergency rescue plan. The safety degree of the instrumented soil slope will be divided into three levels, which are safety level; very early warning level; and serious warning level.

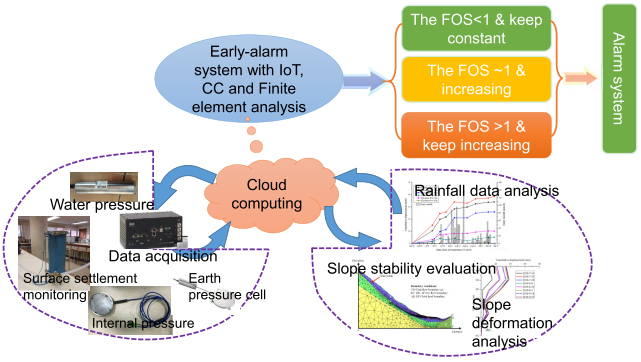

FIGURE 3. The early-warning system of the soil slope which includes a sensing layer, numerical analysis in could computing, and the application layer of with 3 alarm levels (i.e. safety level, caution level, and serious hazard level).

III. A NEW FPS FOR THE SENSING LAYER

A new type of fiber-optic based pressure sensor (FPS) for pressure measurement of earth materials are proposed, fabricated and analyzed for the sensing layer. The working principles, fabricated details and calibration tests are elaborated. A dual diaphragm type fiber-optic based pressure sensor is developed and designed. A series of experimental tests have been performed to examine the relationship between applied pressures and strains induced in FBG sensors. The results along with some findings are presented and discussed.

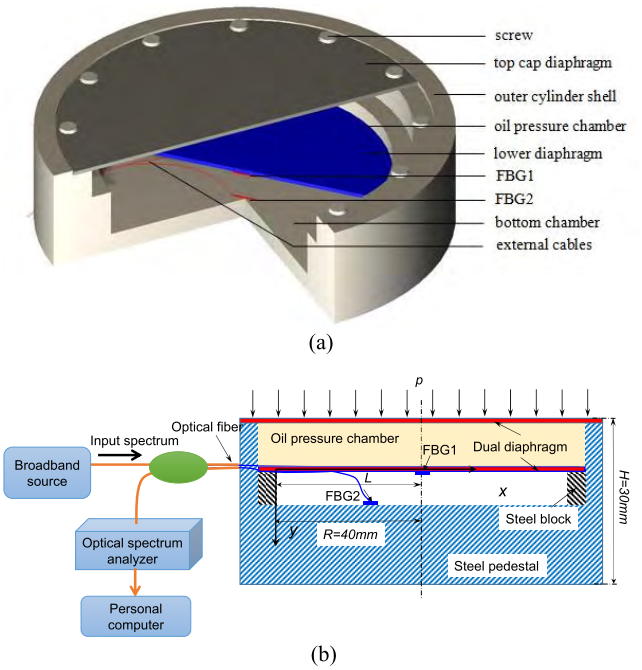

FIGURE 4. Sectional schematic graph of the FPS with dual diaphragm integrated fiber-optic pressure sensor: (a) 3D view; (b) 2D view.

A. PRINCIPLE

A FPS with dual diaphragm is proposed and shown in Fig. 4. By assuming a small strain case and a perfectly elastic material of the diaphragm, when applying an evenly distributed pressure p, the radial strain ε_r and tangential strain ε_t of the diaphragm on the surface can be given as:

$$\varepsilon_t = \frac{3p}{8Et^2}\left(1-\mu^2\right)\left(R^2-r^2\right) \tag{3a}$$

$$\varepsilon_r = \frac{3p}{8Et^2}\left(1-\mu^2\right)\left(R^2-3r^2\right) \tag{3b}$$

where p is the pressure applied on the FPS; E and μ are the Young's modulus and Poisson's ratio; t and R are the thickness and radius of the diaphragm; r is the distance between the measuring point and the center in the horizontal direction. If $r = 0$, then the strains induced in the FBG1 sensor (see in Fig.2b) can be obtained using the following relationship:

$$\varepsilon_{FBG} = \frac{3p}{8Et^2}\left(1-\mu^2\right)R^2 = \frac{p}{C_1} \tag{4}$$

where $C_1 = \frac{8Et^2}{3(1-\mu^2)R^2}$, C_1 represents for the coefficient between the pressure variations and strains measured by the FBG1. It should be noted that the strain measured by FBG1 is in the axial direction only (length wise). Thus, the relationship between the wavelength shift and the pressure applied on the FPS can be obtained:

$$\frac{\Delta\lambda_B}{\lambda_B} = \frac{3c_1}{8Et^2}\left(1-\mu^2\right)R^2\cdot p + c_2\Delta T \tag{5}$$

where c_1 and c_2 are the coefficients from Eq. 4. A separately FBG temperature sensors was installed in the FPS (i.e. FBG2 in this study). The temperature sensor will not endure any external pressures, thus it will be only changed with temperature variations. Therefore the temperature effect can be compensated from Eq. 5. It can be observed that the shift of Bragg wavelength has a close linear relationship with the applied pressure by excluding the temperature effect.

B. DESIGN AND CALIBRATIONS

A prototype of the dual diaphragm FPS was proposed and fabricated in the Civil Engineering laboratory of the Huazhong University of Science and Technology. The FPS consists of a stainless steel outer cylinder shell with 100 mm diameter and 30 mm height. The major components of the FPS include a top cap diaphragm, a lower diaphragm, an oil pressure chamber, a bottom chamber, two FBG sensors and external cables. The thicknesses of both the diaphragms are 0.6 mm. As shown in Fig. 4(a), the whole pressure sensor was firmly assembled with screws to make sure that the two chambers would not be connected and the diaphragms were perfectly clamped on the circumference. FBG1 sensor was glued at the center and on the underside of the lower stainless steel diaphragm, while FGB2 sensor was loosed at the bottom chamber to compensate the temperature effect as the FBG2 only experience temperature variations (Fig. 4(b)). The oil pressure chamber was carefully filled with vacuum grease to ensure no trapped bubbles. Thus, the external force applied to the top cap could be fully transferred and evenly distributed

TABLE 1. The measured strain errors with FBG sensors by simplifying "point" strain.

Length of the FBG sensor	0	4 mm	6 mm	8 mm	10 mm	$k=l/80$
$\Delta\varepsilon$	0	+0.251%	+0.464%	+1.010%	+1.587%	$+k^2/(1-k^2)$

to the lower diaphragm even under the condition of high pressure and temperature. When a pressure was applied on the top cap, the diaphragms were deformed and strained in conjunction with the applied load, the FBG1 sensor was also strained together with the lower diaphragm. By comparing the wavelength shifts of the FBG sensors, a relationship between the diaphragm strain lever and the applied pressure was established.

Prior to the calibration tests, vacuum grease was filled in the dual diaphragm chamber to ensure that no leakage took place during all the tests. The calibration tests were conducted by applying step pressures on the surface of the FPS. Wavelengths of the FBG sensors were recorded during each applied load. Fig. 5(a) shows the spectrum of the FBG sensors. The peak wavelengths were recorded and used to calculate strains by using Eq. 2. Fig. 5(b) and (c) show the wavelengths and strains of the FBG sensors varied with the applied pressures, respectively. Both loading and unloading were tested during the calibration tests. As mentioned before, temperature compensation was conducted by using a separate FBG temperature sensor (i.e. FBG2). Thus, the temperature effect can be eliminated from measured strains by using Eq. 2.

C. DISCUSSIONS

In order to determine the dimension and material of the FPS, a parametric study was carried out and the results are presented in Fig. 6. The results indicate that the resolution of the FPS decreases with the thickness and Young's modulus of the diaphragm, while the resolution increases with the radius of the diaphragm. The results indicate a smaller Young's modulus also yields a finer resolution. The minimum resolution ranges between 1 mm to 2 mm for the diaphragm with a Young's modulus of 200 GPa.

The dual diaphragm type FPS is demonstrated to have the capability of monitoring the applied pressure within a fair degree of accuracy. As indicated in Fig.5, the average sensitivity of the FPS with dual diaphragm is 0.124 kPa/$\mu\varepsilon$. The sensitivity from theoretical analysis is 0.1287 kPa/$\mu\varepsilon$ according to Eq. 4. By considering the fabrication errors, the calibration results match well with the theoretical value.

The linear relationship between the measured strains of FBG sensors and applied pressures (refer to Eq.4) is based on the assumption that the FBG1 measures a point strain at the central of the diaphragm. However, if the Bragg length of the FBG sensor ranges from 3 mm to 10 mm, the measured strain with the FBG sensor is an average value over the Bragg length. The length of the FBG sensors induced measurement errors are listed in Table. 1. As shown in Table 1, if the Bragg length l is k times the diameter of the diaphragm D, the measurement errors $\Delta\varepsilon = (\varepsilon_{FBG}-\varepsilon_{mean-FBG})/\varepsilon_{mean-FBG}$ will yield $k^2/(1-k^2)$. In this study, the $l/D = 0.12$, the strain measurement error is 1.5%.

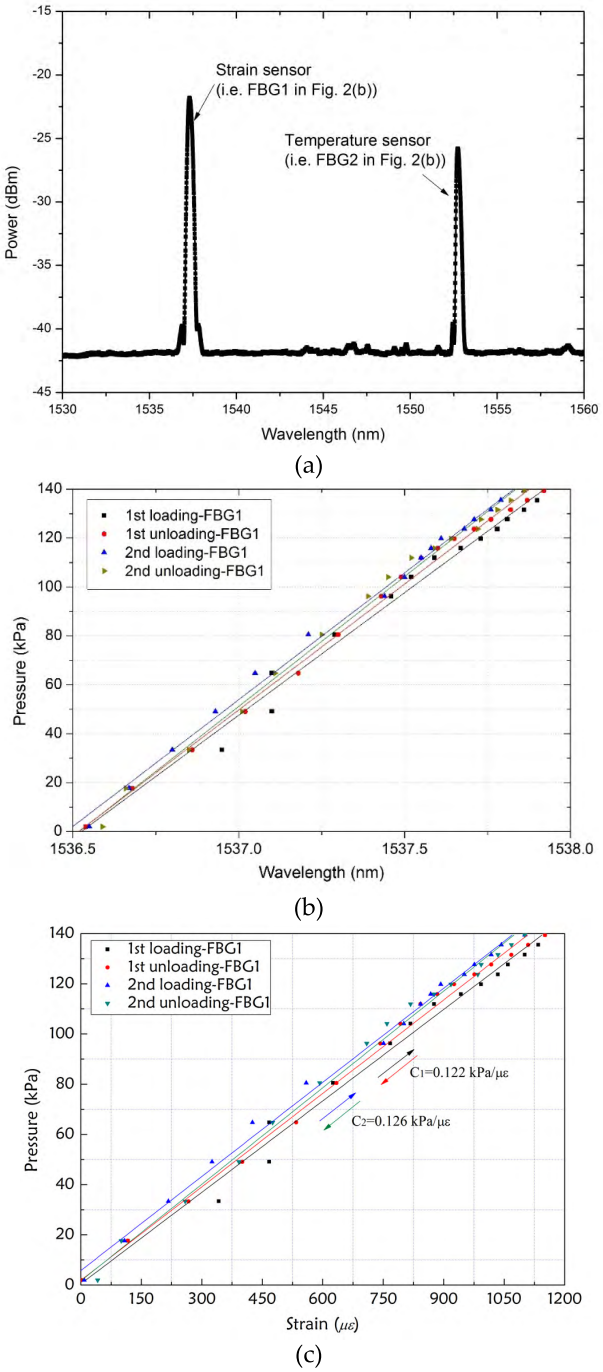

FIGURE 5. The calibration results of FPS with dual diaphragm: (a) the spectrum of the FBG sensors; (b) relationship between wavelengths of the FBG sensors and the applied pressures; (c) relationship between strains of the FBG sensor and applied pressures.

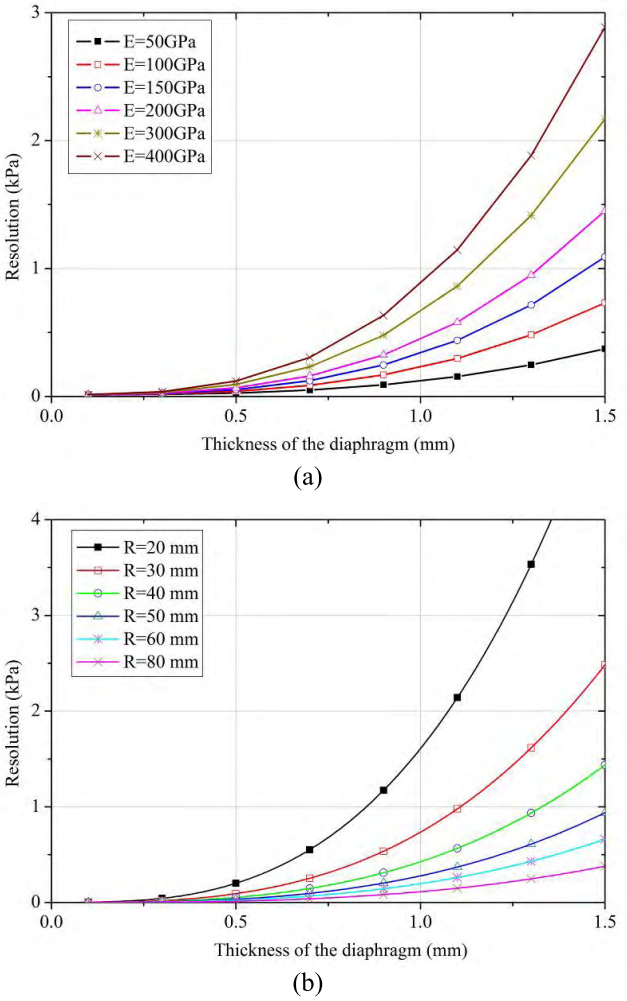

FIGURE 6. Resolution of the designed FPS with various thickness and (a) Young's modulus, and (b) radius of the diaphragm.

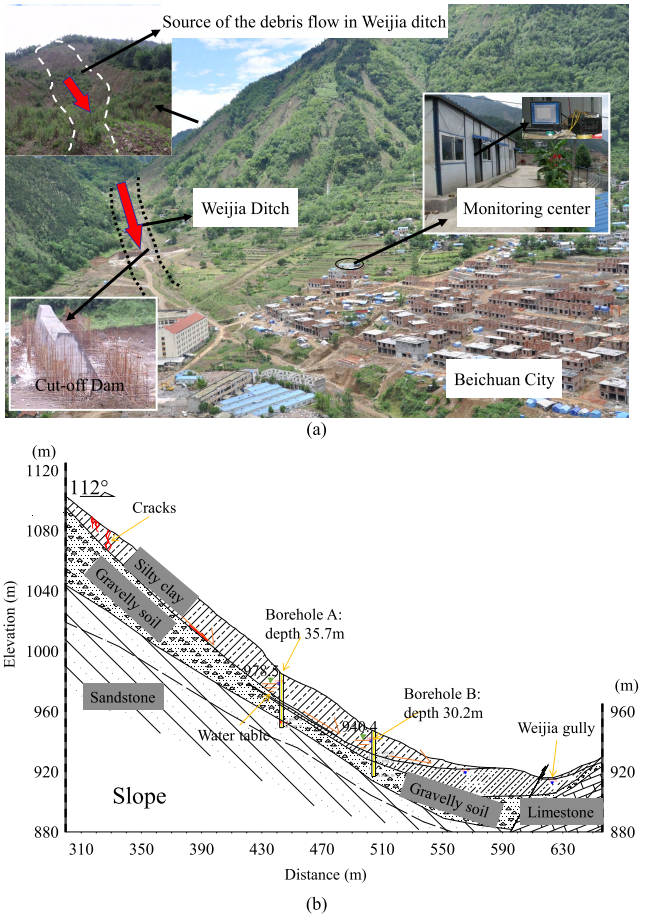

FIGURE 7. The diagram of the instrumented slope: (a) the early-warning system of slope which is the source of debris flow; (b) the sketch the slope consists of sandstone, gravel soil, silt clay.

IV. A CASE STUDY AND DISCUSSION

A fiber optic sensor network was instrumented in a field soil slope. The field geology conditions, sensor deployment, monitoring points and data analysis are presented in this section. Fig. 7 shows the diagram and geology conditions of the instrumented slope. The slope was located in Sichuan, China which is the source of landslides occurred after the ''Wenchuan earthquake'' (12 May 2008) and a heavy rainfall (173.8mm/day). In order to provide safety insurances of the slope stability, an early-warning system with optical fiber sensors were established to monitor the deformation of slope body in different depths.

A newly developed fiber optic based pressure sensors and displacement sensors were installed in bore holes of the slope (Fig. 7). The fiber optic sensors in the sensing layer were connected through one fiber optic cable. Then, all the transducers in the sensing layer were connected with the data acquisition system. The internal deformation of the soil slope is resulted from the earth pressure. Thus, the deformation is a direct indicator for slope stability. Fig. 8 shows the slope movement at different depths during a half year. The depth is the vertical distance between fiber optic sensors and the surface of the slope. Measured rainfall data was also presented in the figure. It can be found that the daily rainfall has a strong effect on the slope movement. The slope moved quickly at the heavy rainfall in the period from July 26 to August 22, 2010. The soil movement at slope surface moved is fast than that in the deeper depth.

In the cloud computing platform, a numerical analysis model was used to analyze the slope stability. Rainfall infiltration is an essential factor which should be incorporated in the numerical analysis. The FOS was calculated under different rainfall intensity and durations. The rainfall data will be further used in the slope stability analysis which was carried out in the software SEEP/W and SLOPE/W [29] based on the geology conditions presented in Fig. 7. A numerical analysis result based on the measured data from the sensing layer is shown in Fig. 9.

The rainfall infiltration will decrease the stability of the slope. Through IoT and cloud computing, it reveals that the slope stability decreases significantly when there is a heavy rainfall with intensity higher than 0.5mm/h and duration is

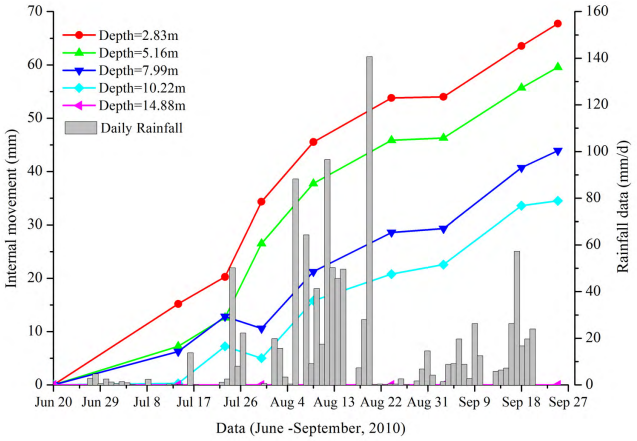

FIGURE 8. Results of slope movement and rainfall data from the sensing layer.

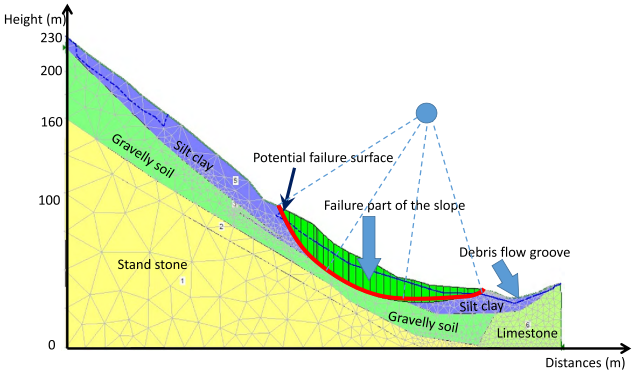

FIGURE 9. Prediction results of slope stability in the cloud computing platform layer.

longer than 100h. Thus, it can be concluded that an early-warning should be triggered and send to the ender users when there is a heavy rainfall with intensity higher than 0.5mm/h and rainfall duration longer than 100h.

V. CONCLUDING REMARKS

The earthquake and rainfall will result in slope failure or debris flow. It is important to develop an early-warning system based on various sensors, IoT and cloud computing. In this study, various fiber optic sensors were installed in a slope. Through IoT and cloud computing, the health condition of the instrumented slope can be evaluated and the analysis results are sent out through the application layer. The major findings are listed as follows.

1) In the sensing layer, the fiber optic sensor is an ideal sensor for small deformation monitoring. A design of FPS with dual diaphragm type was examined and tested. The results indicate that the measured FBG strain has a linear relationship with the applied pressure and the FPS can reach a sensitivity of 0.124 kPa/$\mu\varepsilon$ across the range of 140 kPa. Calibrations results of the FPS with dual diaphragm type indicated that its accuracy can fulfill the requirement of field slope monitoring.
2) The wireless network and optical fibers can be used to connect sensing layer with the data acquisition system. With the IoT, the information of slope deformation will be uploaded to the cloud computing layer.
3) Through IoT and cloud computing, it can be found that the rainfall infiltration strong affect the slope stability, especially on the surface of the slope. The influence decreased dramatically for the depths beyond 5.2m.
4) In the cloud computing layer, a finite element simulation demonstrated that the slope will be collapse when the rainfall higher than 0.5mm/h with rainfall duration larger than 100 h. The analysis results provide a basis for the early-alarm monitoring system.

REFERENCES

[1] L. Zan, G. Latini, E. Piscina, G. Polloni, and P. Baldelli, "Landslides early warning monitoring system," in *Proc. IEEE Int. Geosci. Remote Sens. Symp.*, vol. 1. Jun. 2002, pp. 188–190, doi: 10.1109/IGARSS.2002.1024983.

[2] L. Dong, W. Shu, D. Sun, X. Li, and L. Zhang, "Pre-alarm system based on real-time monitoring and numerical simulation using Internet of Things and cloud computing for tailings dam in mines," *IEEE Access*, vol. 5, pp. 21080–21089, 2017, doi: 10.1109/ACCESS.2017.2753379.

[3] T. M. Sarath, J. P. SubhaHency, and F. Daniel, "Level measurement using MEMS pressure sensor," *Int. J. Adv. Res. Comput. Sci. Softw. Eng.*, vol. 3, pp. 118–121, Jan. 2013.

[4] B.-Y. Lee, J. Kim, H. Kim, C. Kim, and S.-D. Lee, "Low-cost flexible pressure sensor based on dielectric elastomer film with micro-pores," *Sens. Actuators A, Phys.*, vol. 240, pp. 103–109, Apr. 2016.

[5] C.-L. Cheng, H.-C. Chang, C.-I. Chang, Y.-T. Tuan, and W. Fang, "Mechanical force-displacement transduction structure for performance enhancement of CMOS-MEMS pressure sensor," in *Tech. Dig., 27th IEEE Int. Conf. Micro Electro Mech. Syst. (MEMS)*, San Francisco, CA, USA, Jan. 2014, pp. 757–760.

[6] C.-L. Cheng, H.-C. Chang, C.-I. Chang, and W. Fang, "Development of a CMOS MEMS pressure sensor with a mechanical force-displacement transduction structure," *J. Micromech. Microeng.*, vol. 25, no. 12, p. 125024, 2015.

[7] M. Shahiri-Tabarestani, B. A. Ganji, and R. Sabbaghi-Nadooshan, "Design and simulation of high sensitive capacitive pressure sensor with slotted diaphragm," in *Tech. Dig., Int. Conf. Biomed. Eng. (ICoBE)*, Penang, Malaysia, Feb. 2012, pp. 484–489.

[8] W.-C. Lin, C.-L. Cheng, C.-L. Wu, and W. Fang, "Sensitivity improvement for CMOS-MEMS capacitive pressure sensor using double deformarle diaphragms with trenches," in *Proc. 19th Int. Conf. Solid-State Sens., Actuators Microsyst.*, Kaohsiung, Taiwan, Jun. 2017, pp. 782–785.

[9] C. C. Lai, H. Y. Au, M. S. Y. Liu, S. L. Ho, and H. Y. Tam, "Development of level sensors based on fiber Bragg grating for railway track differential settlement measurement," *IEEE Sensors J.*, vol. 16, no. 16, pp. 6346–6350, Aug. 2016.

[10] K. O. Hill and G. Meltz, "Fiber Bragg grating technology fundamentals and overview," *J. Lightw. Technol.*, vol. 15, no. 8, pp. 1263–1276, 1997.

[11] G. Rajan, Ed., *Optical Fiber Sensors: Advanced Techniques and Applications*. Boca Raton, FL, USA: CRC Press, 2015.

[12] T. Guo *et al.*, "Temperature-insensitive fiber Bragg grating liquid-level sensor based on bending cantilever beam," *IEEE Photon. Technol. Lett.*, vol. 17, no. 11, pp. 2400–2402, Nov. 2005.

[13] K.-R. Sohn and J.-H. Shim, "Liquid-level monitoring sensor systems using fiber Bragg grating embedded in cantilever," *Sens. Actuator A, Phys.*, vol. 152, no. 2, pp. 248–251, Jun. 2009.

[14] B. Yun, N. Chen, and Y. Cui, "Highly sensitive liquid-level sensor based on etched fiber Bragg grating," *IEEE Photon. Technol. Lett.*, vol. 19, no. 21, pp. 1747–1749, Nov. 1, 2007.

[15] C. Yang, S. Chen, and G. Yang, "Fiber optical liquid level sensor under cryogenic environment," *Sens. Actuators A, Phys.*, vol. 94, nos. 1–2, pp. 69–75, Oct. 2001.

[16] K. Bremer *et al.*, "Fibre optic pressure and temperature sensor for geothermal wells," in *Proc. IEEE SENSORS*, Kona, HI, USA, Nov. 2010, pp. 538–541.
[17] K. Bremer, E. Lewis, G. Leen, B. Moss, S. Lochmann, and I. A. R. Mueller, "Feedback stabilized interrogation technique for EFPI/FBG hybrid fiber-optic pressure and temperature sensors," *IEEE Sensors J.*, vol. 12, no. 1, pp. 133–138, Jan. 2011.
[18] T. Reinsch *et al.*, "A fibre optic sensor for the *in situ* determination of rock physical properties," *Int. J. Rock Mech. Mining Sci.*, vol. 55, pp. 55–62, Oct. 2012. [Online]. Available: https://doi.org/PP10.1016/j.ijrmms.2012.06.011
[19] L.-J. Dong, J. Wesseloo, Y. Potvin, and X.-B. Li, "Discriminant models of blasts and seismic events in mine seismology," *Int. J. Rock Mech. Mining Sci.*, vol. 86, pp. 282–291, Jul. 2016.
[20] L. Dong, J. Wesseloo, Y. Potvin, and X. Li, "Discrimination of mine seismic events and blasts using the Fisher classifier, naive Bayesian classifier and logistic regression," *Rock Mech. Rock Eng.*, vol. 49, no. 1, pp. 183–211, Jan. 2016.
[21] L. Dong, W. Shu, X. Li, G. Han, and W. Zou, "Three dimensional comprehensive analytical solutions for locating sources of sensor networks in unknown velocity mining system," *IEEE Access*, vol. 5, pp. 11337–11351, 2017.
[22] G. Han, L. Liu, S. Chan, R. Yu, and Y. Yang, "HySense: A hybrid mobile crowdsensing framework for sensing opportunities compensation under dynamic coverage constraint," *IEEE Commun. Mag.*, vol. 55, no. 3, pp. 93–99, Mar. 2017.
[23] R. Liu and J. Wang, "Internet of Things: Application and prospect," in *Proc. MATEC Web Conf.*, Zhengzhou, China, 2017, Art. no. 02034.
[24] G. Han, L. Liu, J. Jiang, L. Shu, and G. Hancke, "Analysis of energy-efficient connected target coverage algorithms for industrial wireless sensor networks," *IEEE Trans. Ind. Informat.*, vol. 13, no. 1, pp. 135–143, Feb. 2017.
[25] G. Han, J. Jiang, C. Zhang, T. Q. Duong, M. Guizani, and G. K. Karagiannidis, "A survey on mobile anchor node assisted localization in wireless sensor networks," *IEEE Commun. Surveys Tuts.*, vol. 18, no. 3, pp. 2220–2243, 3rd Quart., 2016.
[26] G. Han, J. Jiang, M. Guizani, and J. J. P. C. Rodrigues, "Green routing protocols for wireless multimedia sensor networks," *IEEE Wireless Commun.*, vol. 23, no. 6, pp. 140–146, Dec. 2016.
[27] D.-S. Xu, "Development of two optical fiber sensing technologies and applications in monitoring geotechnical structures," Ph.D. dissertation, Dept. Civil Environ. Eng., Hong Kong Polytech. Univ., Hong Kong, 2014.
[28] *Seep/W User's Guide for Finite Element Seepage Analysis*, GEO-SLOPE Int. Ltd., Calgary, AB, Canada, 2004.

DONG-SHENG XU received the M.Eng. degree in geotechnical engineering from the Chinese Academy of Sciences, China, and the Ph.D. degree from The Hong Kong Polytechnic University, with a focus on the development of FBG and BOTDA sensors. He is currently an Assistant Professor of civil engineering with the Huazhong University of Science and Technology, China. His research interests include the development of various optical fiber sensors and ultrasonic sensors for civil infrastructures.

LONG-JUN DONG received the Ph.D. degree from the School of Resources and Safety Engineering, Central South University, Changsha, China, in 2013. From 2012 to 2013, he was an Assistant Researcher with the Australia Center for Geomechanics, The University of Western Australia, Perth, Australia. He is currently an Associate Professor with the School of Resources and Safety Engineering, Central South University. His current research interests include computational methods in location and identification for shock sources, seismic signals, machine learning algorithms, and rock/mineral mechanics for mining science. He is a member of the ASCE and ISRM. He has served as a reviewer for over 30 journals. He was selected for the Young Elite Scientists Sponsorship Program by the China Association for Science and Technology. He is invited to serve as the Editorial Board Member of the *Scientific Reports*, the *Internal Journal of Distributed Sensor Networks*, and *Shock and Vibration*.

LALIT BORANA received the B.Eng. degree in civil engineering from the Visvesvaraya Technological University, Belgaum, in 2006, the M.Tech. degree in geotechnical engineering from IIT Guwahati in 2008, and the Ph.D. degree in geotechnical engineering from The Hong Kong Polytechnic University in 2014. He is currently an Assistant Professor with the IIT Indore, Indore, India. His current research interests involve fiber optic sensors and structural health monitoring.

HUA-BEI LIU received the M.Eng. degree from Columbia University and the Ph.D. degree from Tsinghua University. He is currently a Full Professor of geotechnical engineering with the Huazhong University of Science and Technology, China. His research interests consist of civil infrastructure safety analysis and control.